

# Neutral ion figuring of chemical vapor deposited SiC

**Steven C. Fawcett**

National Aeronautics and Space  
Administration  
Marshall Space Flight Center  
Optical Systems Branch, EB53  
Huntsville, Alabama 35812  
E-mail: fawcett@zeus.msfc.nasa.gov

**Thomas W. Drueding**

**Thomas G. Bifano**

Boston University  
Aerospace and Mechanical Engineering  
110 Cummington Street  
Boston, Massachusetts 02215

**Abstract.** Ion figuring of optical components is a relatively new technology that can alleviate some of the problems associated with traditional contact polishing. Because the technique is noncontacting, edge distortions and rib structure print through do not occur. This investigation was aimed at determining the effect of ion figuring on surface roughness of previously polished or ductile ground ceramic optical samples. This is the first step in research directed toward the combination of a prefinishing process (ductile grinding or polishing) with ion figuring to produce finished ceramic mirrors. Multiple, chemical vapor deposited silicon carbide (CVD SiC) samples were polished or ductile ground to specular or near-specular roughness. These samples were then characterized to determine topographic surface information. The surface evaluation consisted of stylus profilometry, interferometry, and optical and scanning electron microscopy. The surfaces were then ion machined to depths from 0 to 5  $\mu\text{m}$ . The finished surfaces were characterized to evaluate the effects of the ion-machining process with respect to the previous processing methods and the preexisting subsurface damage. This study provides some of the information required to effectively utilize a combined ductile grinding or polishing with ion machining as a procedure for figuring optical components.

*Subject terms:* silicon carbide; ion figuring; optical fabrication; ductile grinding; polishing.

*Optical Engineering* 33(3), 967–974 (March 1994).

## 1 Introduction

A new precision fabrication facility is currently being implemented at the National Aeronautics and Space Administration's (NASA's) Marshall Space Flight Center (MSFC). One of the technologies that is being evaluated to complement the traditional high-precision material removal techniques is ion figuring. The use of neutral ion beams to remove selected material has been developed and is currently in use at commercial installations and research facilities.<sup>1–10</sup> These implementations typically use the process for final figure correction on meter-class optical components. The new facility at MSFC will focus on evaluating and developing this technique for producing the optics required on many of NASA's missions. The initial work will focus on the production of centimeter-

scale optics to achieve the extremely tight tolerances in a reasonable time. After the development work has been completed, the fabrication procedures will be optimized for the particular requirements of various missions. The fabrication test program currently underway includes polishing or ductile-regime grinding to obtain good surface finish followed by neutral ion beam machining to produce good figure accuracy.

## 2 Polishing and Ductile Regime Grinding

Loose abrasive polishing and ductile regime grinding are two fabrication processes that can provide optical quality surface finish on a glass or ceramic mirror—a necessary preparation for subsequent ion figuring. Polishing usually involves loose abrasive particles working between a flexible pad and the mirror material, creating the desired surface characteristics by either frictional abrasion or chemical reactions or both. A newer fabrication procedure that can potentially be used for optical surface fabrication is ductile regime grinding.<sup>11–14</sup>

Paper 05043 received April 7, 1993; revised manuscript received June 5, 1993; accepted for publication June 6, 1993.  
© 1994 Society of Photo-Optical Instrumentation Engineers. 0091-3286/94/\$6.00.

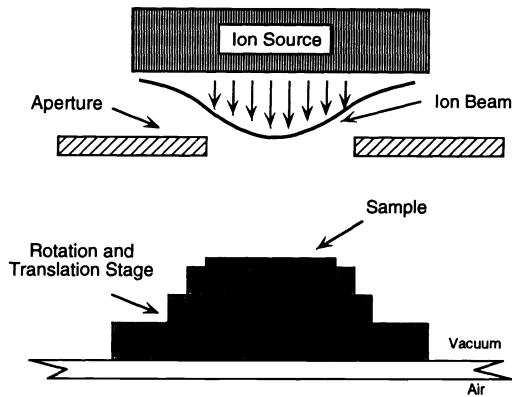


**Fig. 1** Schematic of ion figuring process. A semi-Gaussian ion function imparts the final figure contour on the substrate by computer-controlled translation and rotation.

In this technique, the substrate is formed on a precisely controlled fixed-abrasive grinding machine. The process parameters are controlled to allow for material removal by plastic deformation instead of brittle fracture. Both polishing and ductile grinding can produce the angstrom-level surfaces required by precision optical components. Note that the ion figuring technique requires that the mirror segments have optical quality surface finishes prior to figuring because the ion machining cannot currently be utilized to improve the finish of components. Polishing and ductile-regime grinding will be evaluated as preliminary fabrication technologies, in which the contour accuracy of the component is achieved to within 1 to 2  $\mu\text{m}$  of the final specification, and the component is finished to the final surface roughness specification. Subsequent ion figuring will then be used to improve the contour accuracy while maintaining angstrom-level roughness.

### 3 Neutral Ion Figuring

The use of neutral ion beams to remove selected material has been developed for final figure correction on meter-class optical components.<sup>5-8</sup> The technique has been developed for this size application with commercially available, 3- to 5-cm ion sources. These sources are utilized for the correction of large and middle spatial frequency errors on these meter-size components. The procedure uses an interferometric contour map subtracted from an ideal contour map to produce a map of the figure errors. The process itself is based on a momentum transfer from previously ionized molecules of inert gas. This results in molecular-level sputtering of the substrate material. The basic operation is depicted in Fig. 1.

The new research facility at MSFC will focus on using the technique for the figuring of centimeter-scale optics.<sup>15</sup> This facility was constructed around a surplus sputtering chamber obtained for this program. This chamber was retrofitted with a 3-cm, Kaufman filament type ion source<sup>16</sup> from Ion Tech Incorporated.<sup>16</sup> This source is driven by a programmable power supply that can provide current densities to 10 mA/cm<sup>2</sup>. The basic system is shown in the computer model of Fig. 2.

The experiments were designed to evaluate the machining characteristics of chemical vapor deposited silicon carbide (CVD SiC). The CVD SiC samples used in these experiments were obtained from Morton International, Advanced Materials, and were 3 mm thick. The polished samples were 3-

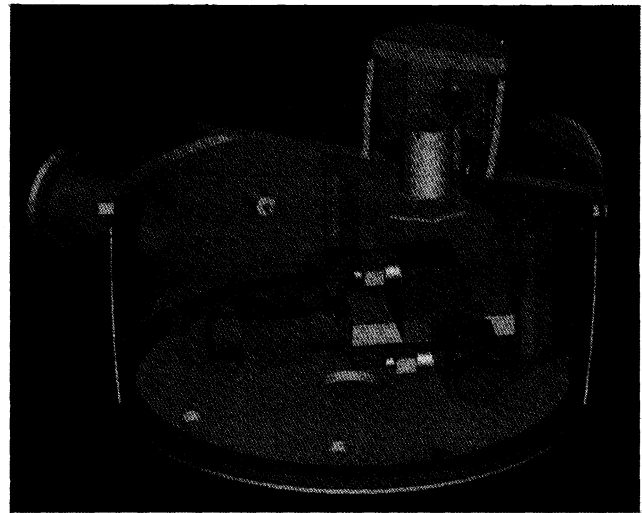


**Fig. 2** Solid model of the ion-figuring system components. The ion source is supported on two posts above the translation/rotation stage assembly. These components are housed in a 1-m-diam, cylindrical vacuum chamber.

**Table 1** CVD SiC polishing parameters.

Sample	Time	Grit Size
P1	10 min	1/2 $\mu\text{m}$
P2	35 min	1/2 $\mu\text{m}$
P3	40 min	1/2 $\mu\text{m}$
P4	60 min	1/2 $\mu\text{m}$

cm-diam circular pieces and the ductile ground samples were 6-mm-wide  $\times$  25-mm-long rectangular pieces. The polished samples were processed by lapping with an oil-based diamond compound. The lapping was done in steps starting with 15- $\mu\text{m}$  diamond and proceeding through 9, 6, 3, and 0.5  $\mu\text{m}$ . The processing continued only as long as required to remove the visible scratches from the previous steps. The final polishing at the smaller grit sizes on the four polished samples was continued for the times and grit sizes listed in Table 1.

The ductile ground CVD SiC samples were obtained from the same batch as the polished samples. They were mounted on steel sample holders and ground in the ductile regime. The grinding was performed by Yuan Yi at the Boston University Precision Engineering Research Laboratory. A 4- to 8- $\mu\text{m}$  resin-bonded diamond abrasive in a wheel running at 3600 rpm with deionized water coolant was used for samples D2, D3, and D4. Sample D1 was ground using a 180- $\mu\text{m}$  bronze bond diamond abrasive wheel. The larger grit wheel, in combination with more aggressive infeed and crossfeed rates, was expected to cause several micrometers of subsurface damage in the silicon carbide workpiece D1. The grinding parameters for each sample are summarized in Table 2.

### 4 Machining Depth

An experiment was performed to determine the beam current profile and hence the expected material removal rate on the CVD SiC samples. In this experiment, a polished, circular sample was located beneath the ion beam so that the edge of

**Table 2** CVD SiC grinding parameters (D1 was ground in the brittle regime, whereas D2 to D4 were ground in the ductile regime).

Sample	Passes	Infeed	Crossfeed Rate
D1	7	250 nm	5.5 $\mu\text{m}/\text{rev}$
D2	7	200 nm	5.5 $\mu\text{m}/\text{rev}$
D3	6	200 nm	3.8 $\mu\text{m}/\text{rev}$
D4	5	250 nm	3.8 $\mu\text{m}/\text{rev}$

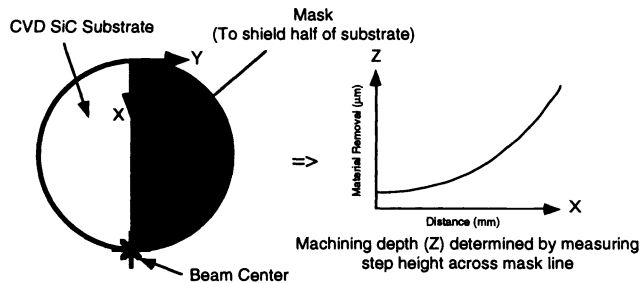


**Fig. 3** Masking technique for determining machining rate.

**Table 3** Ion source operating parameters.

Parameter	Value
Cathode Current	4.3 A
Discharge Current	0.6 A
Discharge Voltage	40 V
Beam Current	40 mA
Beam Voltage	1000 V
Accelerator Current	2 mA
Accelerator Voltage	150 V
Neutralizer Current	50 mA
Filament Current	4.1 A
Source Distance	8 cm
Pressure	$1.4 \times 10^{-4}$ torr

the sample would correspond with the point of maximum beam intensity. One half of the sample was masked to provide a reference surface for step-height measurements. This process is depicted in Fig. 3. Throughout these experiments, the ions were produced from argon gas with the parameters listed in Table 3. After the sample was ion machined for a specified period, the relative height differences between the surfaces was measured with a Talysurf stylus profilometer and normalized with respect to time. Figure 4 shows a plot of the measured machining rate versus the distance from the beam center. This Gaussian profile was used to provide varying depths of material removal for the surface characterization study.

## 5 Surface Characterization

Once the samples were polished or ground, surface characterization measurements were made. Unmagnified, visual examination revealed no scratches or pits in any of the samples. Optical microscopy to  $400\times$  only revealed an occasional

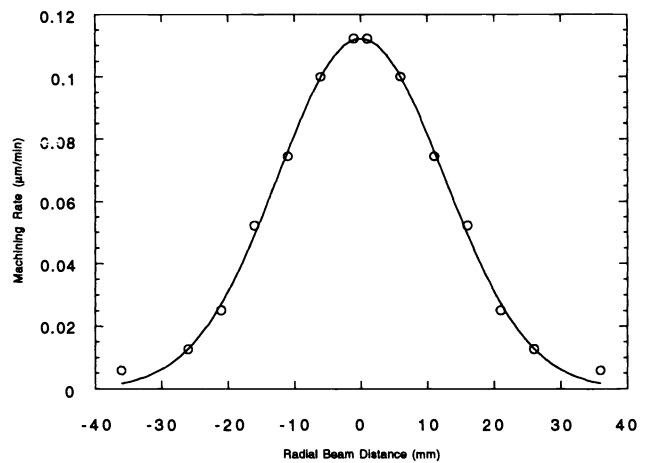


**Fig. 4** Machining profile of 3-cm ion source.



**Fig. 5** SEM micrograph of the polished CVD SiC samples at 2000X.

fracture location and grooves on the ground samples caused by the grinding crossfeed, especially on sample D1. The samples were viewed with a scanning electron microscope (SEM). These pictures are shown in Figs. 5 and 6 and again reveal the grinding crossfeeds and occasional fracture sites. There were small ( $\approx 100$ - to  $200$ -nm-diam) discontinuities visible in the SEM micrographs of the ground samples. On all the polished samples, small ( $\sim 100$  nm wide) scratches became visible.

All the samples were measured to determine the surface roughness parameters prior to ion machining. It was determined that the surface roughness of the samples was below the noise floor of the Talysurf profilometer. The initial measurements were instead made on a WYKO optical profilometer to determine the surface roughness. Ductile ground sample D4 was also measured by Mark Gerchman of Rank Taylor Hobson, Inc., on a Talystep stylus profilometer for verification. Multiple measurements were made for each sample and the results averaged. The rms values from the WYKO data for an area approximately  $235 \times 235 \mu\text{m}$  square ranged from  $7.56 \pm 2.07$  to  $12.77 \pm 4.65 \text{ \AA}$  for the polished samples and from  $12.87 \pm 4.94$  to  $52.25 \pm 34.51 \text{ \AA}$  for the ductile ground samples. The Talystep data for sample D4 gave an

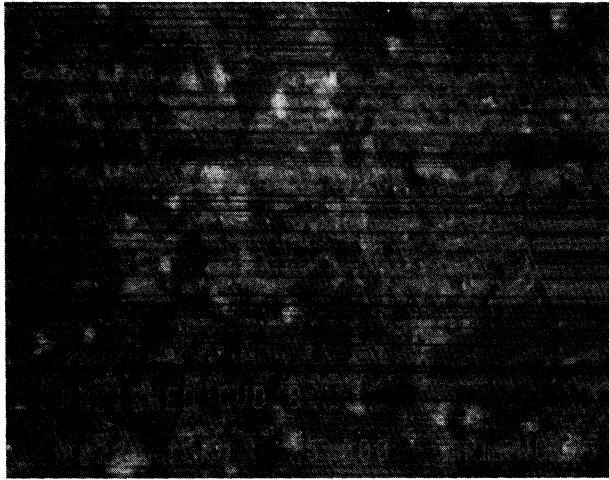


**Fig. 6** SEM micrograph of the ductile ground CVD SiC samples at 5000X (caption reading "POLISHED" is incorrect).

average roughness of  $13.14 \pm 5.24 \text{ \AA}$  rms for a 150- $\mu\text{m}$  linear trace.

## 6 Results

After the initial surface finish evaluation, the samples were ion machined in a fixed position with respect to the beam, so that the total depth profile at various positions on the sample surface could be correlated with the ion-machining depth profile plotted in Fig. 4. These samples were then examined to determine the effect of the ion-sputtering process. During machining, the samples could be viewed through a transparent port in the vacuum chamber. This examination revealed an interesting phenomenon: previously hidden damage on the polished samples (and, to a lesser extent, on the ground samples) became highly visible after only a few minutes under the beam. After machining, some of the samples showed extensive damage when examined under an optical microscope. The extent of this damage increased with an increase in ion-machining depth. Figure 7 shows the extent of the damage incurred on sample P1 at various machining depths.

Optical micrographs revealed hemispherical pits uncovered by the ion-machining process on the polished samples. The pits are believed to have been formed at the sites of subsurface damage caused by the loose abrasive polishing with the larger grit diamond. The size of the pits is approximately 10 to 20  $\mu\text{m}$  diameter, which corresponds to the fracture size expected from the initial polishing stage with 15- $\mu\text{m}$  diamond. Because of the lack of a controlled polish, it is probable that the fractures from previous grit sizes were not completely removed in subsequent steps and were left as subsurface damage. These damage sites were then uncovered by the ion figuring.

The almost perfect hemispherical shape of these pits initially led the investigators to believe that these features were actually redeposited material that coalesced on the substrate. Figure 8 is a Talysurf trace of sample P1 that clearly reveals that the features are pits ranging to 1.6  $\mu\text{m}$  in depth. The micrograph of Figs. 9 and 10 appear to verify the hypothesis that the pits are formed in the areas of subsurface fracture. Figure 9 shows a line of these hemispherical pits formed on

an uncovered subsurface scratch. These pits apparently follow a scratch line where fractures occur under the stresses induced while polishing with the larger grit sizes. The magnified view in Fig. 10 shows the hemispherical nature of the pits.

It is believed that the pitting sites are formed when the lateral cracks caused by the forces of the individual diamond grits are uncovered. The lateral cracks may potentially propagate because of the removal of the plastic flow layer that initially provided the stresses required to maintain equilibrium. Figure 11 demonstrates this idea schematically. When the plastic layer is removed by the ion-sputtering process, the equilibrium condition is modified by removal of the compressive surface layer with the resulting increase in tensile stress below the surface, and the cracks grow. When the surface layer meets the extended lateral crack, the material above the crack is expelled (releasing the residual stress) to reveal the hemispherical pits. The thermal loading inherent with the ion-figuring process may be a contributing factor. The areal density of these fracture sites appears to directly correlate with the density of the ion beam current and hence with the machining depth.

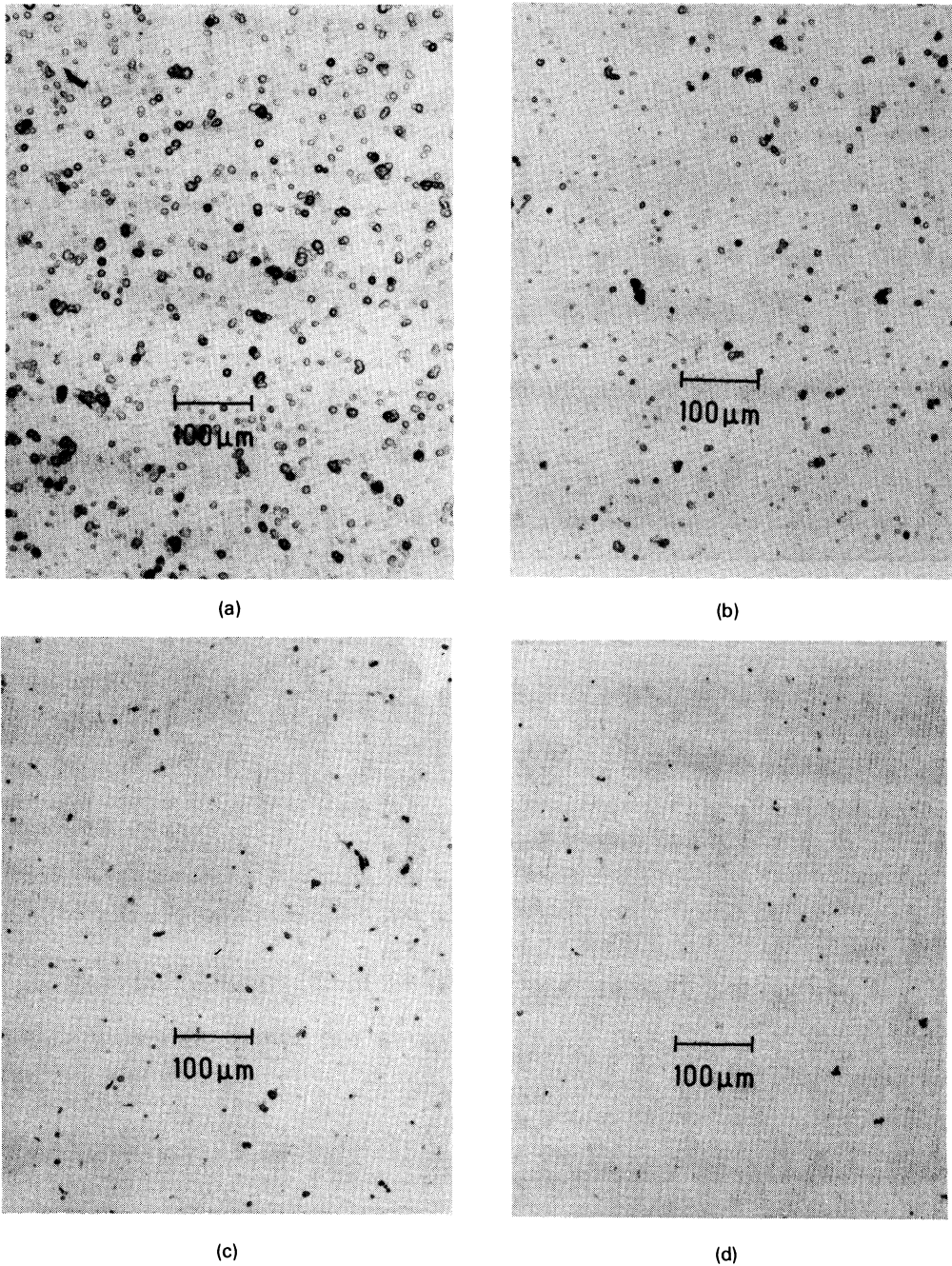
The ground samples were also evaluated optically. The samples ground in the ductile regime showed only a few fracture sites in localized areas of the samples. These areas appeared to correspond with sites that may have undergone some scratching during the grind. An example of such a site is shown in Fig. 12. However, most of the areas were free of fracture and looked similar to the bottom portion of the photo depicted in Fig. 12. The pits shown range from 3 to 8  $\mu\text{m}$  in diameter, which is similar to the diamond grit size of 4 to 8  $\mu\text{m}$ . The brittle ground sample D1 showed some hemispherical pitting similar to what was shown in Fig. 10 for the polished sample.

Surface roughness measurements were also made on the figured samples. Prior to machining, six measurements were made at random locations for each of the samples with the WYKO optical profilometer. These results were averaged and are shown in Table 4.

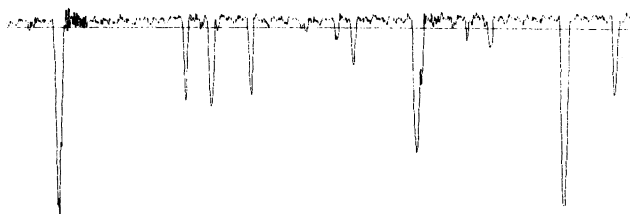
After ion machining, the samples were again measured with the optical profilometer. The total ion machining times for each sample are shown in Table 5. Those samples exhibiting significant pitting (including all of the polished samples and two of the four ground samples) could not be measured with the WYKO optical profilometer. The steep slope of the pit edges exceeded the measurement capacity of the optical profilometer. Data was obtained from the WYKO for three of the ground samples that had relatively few pits (ductile ground samples D2, D3, and D4). The rms surface finish measurements made over the entire surface were averaged to obtain  $15.77 \pm 2.14 \text{ \AA}$  for sample D2,  $17.98 \pm 4.06 \text{ \AA}$  for sample D3, and  $23.01 \pm 6.95 \text{ \AA}$  for sample D4. The area of measurement for the samples was approximately  $470 \times 470 \mu\text{m}$  for D2 and  $235 \times 235 \mu\text{m}$  for D3 and D4. The surface roughness revealed no significant increases as a function of machining depth.

Those samples that could not be measured with the optical profilometer were instead measured using a Talysurf stylus profilometer. This data at each ion-machined depth was collected in four linear, 1-mm traces of the samples with no filtering. The rms roughness average of each set of four traces is plotted against ion machining depth in Figs. 13 and 14.

NEUTRAL ION FIGURING OF CHEMICAL VAPOR DEPOSITED SiC



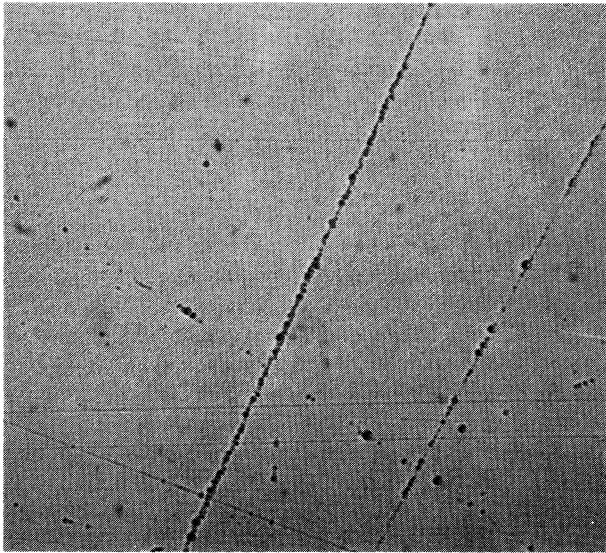
**Fig. 7** Optical micrographs of polished CVD SiC sample P1 ion machined to (a) 5-, (b) 3.2-, (c) 1.8-, and (d) 0.8- $\mu\text{m}$  machining depth.



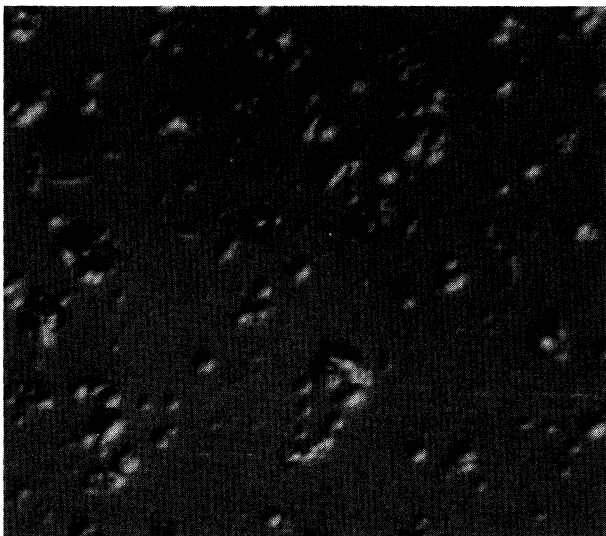
**Fig. 8** Talysurf profile of polished sample P1 after ion machining (P-V approximately 0.9  $\mu\text{m}$ ).

Figure 13 shows the surface roughness as a function of ion machining depth for the polished samples. There is an obvious increase in the surface roughness at the greater machining depths. This roughness increase is primarily due to the pitting that occurred in these polished samples.

Sample P4 does not show the same increase in roughness as the other polished samples. This sample was polished for a longer time than the others, suggesting that the observed pitting may be the result of rough-machining steps prior to polishing, and that the polished samples were not polished long enough to remove all prior damage. Figure 14 shows



**Fig. 9** Optical micrograph of a scratch line revealed by ion machining on a polished CVD SiC sample (200X).



**Fig. 10** Optical micrograph of the subsurface fracture sites uncovered by ion figuring on a polished CVD SiC sample (400X).

the surface roughness measurements for ground sample D1. The other ground samples exhibited roughness that was below the noise floor of the Talysurf profilometer. Sample D1, which was ground in the brittle regime, exhibits the same trend of increasing roughness with ion-machining depth that was observed in the insufficiently polished samples. Before ion machining, D1 had a roughness of 52-Å rms. Also, this sample had an abundance of damage sites that became visible under the optical microscope after ion machining. Note that the vertical resolution of the Talysurf is 10 nm and results in the absence of measurements below this threshold in Figs. 13 and 14. The pitting exhibited on the polished samples and the ground sample D1 prevented Wyko optical profilometry measurements for these samples.

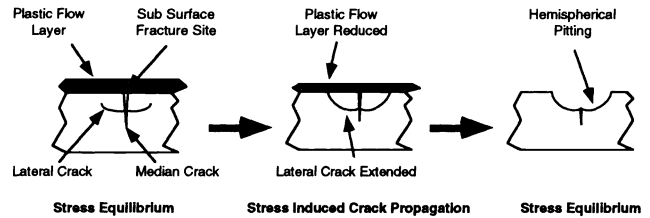


**Fig. 11** Schematic of the proposed crack propagation process. The layer that provided stress equilibrium is removed and the subsurface crack propagates, eventually reaching the surface.

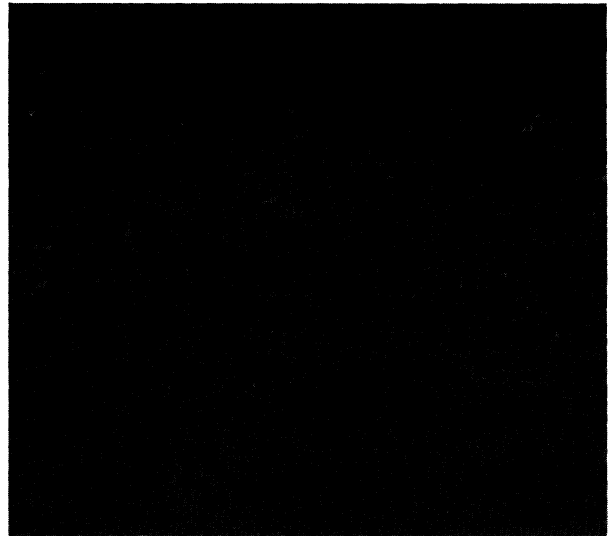


**Fig. 12** Optical micrograph of ductile ground CVD SiC ion machined to a depth of 3 μm (sample D3 at 400X).

## 7 Discussion

From these results, it seems apparent that ion machining acts to expose any preexisting subsurface damage in specularly finished CVD SiC. This exposure of damage causes significant roughening of the surface, diminishing its optical quality. Both prefinishing techniques, grinding and polishing, can be used to generate specular surfaces. However, the roughness of the finished surface is not indicative of the extent of subsurface damage. All of the polished samples, and three of the four ground samples, exhibited rms roughnesses before ion machining that were below 20 Å. After ion machining to a depth of 5 μm, those samples having significant and visually apparent subsurface damage exhibited increases in rms roughness to as much as 1400 Å, whereas those samples that showed no evidence of subsurface damage exhibited almost no increase in rms roughness.

The subsurface damage uncovered by ion machining might have been the result of rough machining processes prior to polishing or grinding, or they might have been introduced by these finishing processes themselves. The evolution of roughness in the polished samples, however, pro-



**Table 4** The rms surface finish of CVD SiC samples (WYKO measurement over an area approximately  $235 \times 235 \mu\text{m}$ ).

Sample	WYKO Data (Å)
P1	7.56+2.07
P2	7.95+0.62
P3	10.5+5.31
P4	12.77+4.65
D1	52.25+34.51
D2	15.78+4.02
D3	12.87+4.94
D4	17.45+2.07

**Table 5** Ion machining time.

Sample	Time
P1	45 min
P2	30 min
P3	35 min
P4	90 min
D1	60 min
D2	45 min
D3	30 min
D4	60 min

vides evidence suggesting that prior machining processes are responsible: the polished sample exhibiting the least amount of subsurface damage had been polished for at least twice as long as the other samples but no verifiable material removal measurements were ever made during the polishing. If the polishing process itself were a primary contributor to the subsurface damage, this sample would have been expected to exhibit at least as much damage as the others. It is perhaps not surprising that the subsurface damage from previous rough machining was not completely removed in the polished samples: the large value of hardness exhibited by SiC causes it to have an exceptionally low polishing rate. For identical conditions of grit size and polishing pad pressure, the Preston coefficient (removal rate per unit time) for SiC has been found<sup>17</sup> to be less than 1/20 that of optical glasses (BK-7 and fused silica). These polishing experiments were conducted with diamond abrasive on a Kemet lap and with  $\text{B}_4\text{C}$  abrasive on a cast iron lap. Although it is possible to increase the polishing rate by polishing at a higher pad pressure, it is also possible that the increased polishing grain loading would itself result in polish-induced subsurface damage.

Ductile-regime grinding appears to be a good way to obtain the two prerequisites for ion machining: a specular finish and the absence of subsurface damage. It has been demonstrated in these experiments that it is possible to grind SiC to rms roughness in the 10 to 20-Å range without introducing any subsurface damage. If the grinding process is not carried out in the ductile regime, however, then the rms roughness of the sample will increase with subsequent ion machining.

An interesting result of these experiments is the observation that ion machining acts to expose subsurface damage in SiC. By itself, this process may be useful as a locally destructive diagnostic technique for evaluating the subsurface damage in a specular component, in the same way that HF

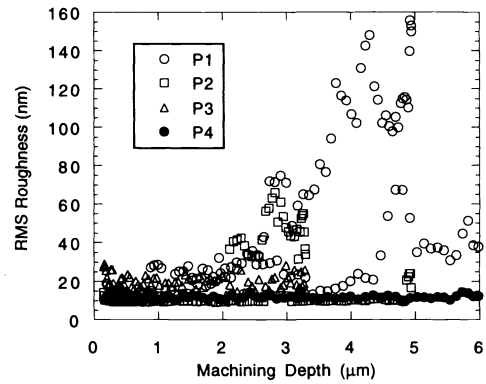


**Fig. 13** Surface roughness variation with ion-machining depth for polished samples.

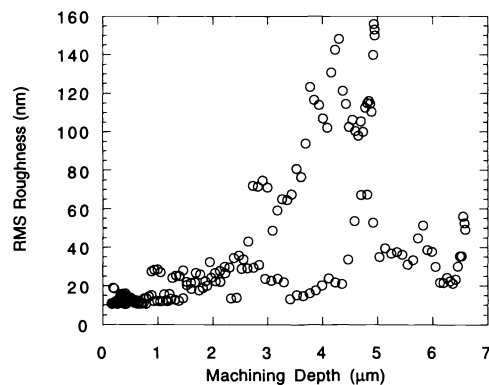


**Fig. 14** Surface roughness variation with ion-machining depth for brittle ground sample D1.

acid etching is used to evaluate subsurface damage in glass. Since acid does not readily etch SiC, ion machining can serve as a clean, efficient alternative for postprocessing measurement of subsurface damage in ceramic components.

These experiments provide strong evidence that ceramic mirrors could be produced by prefinishing in a ductile machining process (either ductile-regime grinding or polishing), followed by ion machining. A distinct advantage of such a fabrication technique is that, at the end of the ion-milling process, the mirror surface is atomically clean, and it is in a vacuum chamber. This means that the surface is ready for any subsequent coating processes that are to be performed on the mirror, processes that generally require atomic cleanliness and a vacuum environment anyway.

## 8 Conclusions

It has been demonstrated that a feasible process for fabricating ceramic mirrors is to employ a deterministic ductile-grinding operation followed by a final ion-beam-contouring operation. A small ion-machining facility has been established, and processing experiments on CVD SiC have been carried out. Removal rates for the ion beam have been characterized. The removal profile is largely Gaussian in shape. CVD SiC samples were polished or micro-ground in preparation for final ion machining. Most of these prefinished samples exhibited roughness in the 10- to 20-Å range. It was found that the

success of the ion-machining process was directly influenced by the existence of subsurface damage: samples containing subsurface damage suffered rapid deterioration in surface quality as a result of the ion machining. The observed subsurface damage in polished samples is likely to be the residual effect of previous machining processes, rather than the direct result of polishing itself. As has been shown in previous work by many researchers, ductile grinding can produce damage-free, optical quality surfaces in SiC. These experiments revealed that high-quality, ductile ground surfaces do not significantly roughen after removal of up to 5  $\mu\text{m}$  of material by ion machining.

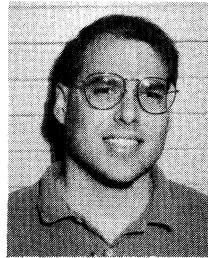
The proposed processing technique shows promise as a viable alternative to conventional fabrication techniques in the production of ceramic mirror components. Moreover, the results of the experiments reported here indicate that ion machining can serve as an indicator of the existence and extent of subsurface damage in specularly finished ceramic components.

### Acknowledgments

This work was sponsored and funded by NASA. The authors would like to express their gratitude to the following people for their support of the project: Robert Rood, James Bilbro, Edward Montgomery, Whit Brantley, Charles Jones, Joseph Randall, and Scott Wilson. Also, special thanks to Charles Griffith and Raj Khanijow who did the tedious job of polishing the samples and to Staffan Persson who designed the support fixtures for the ion source.

### References

1. A. J. Gale, "Ion machining of optical components," in *Optical Society of America Ann. Meet. Conf. Proc.*, pp. (Nov. 1978).
2. J. R. McNeil and W. C. Herrmann, Jr., "Ion beam applications for precision infrared optics," *J. Vac. Sci. Technol.* **20**(3), 324-326 (1982).
3. J. R. McNeil, S. R. Wilson, and A. C. Barron, "Ion beam figuring for rapid optical fabrication," in *Proc. Optical Society of America Wkshp. on Optical Fabrication and Testing*, pp. 62-67 (Oct. 1986).
4. S. R. Wilson, D. W. Reicher, and J. R. McNeil, "Surface figuring using neutral ion beams," in *Advances in Fabrication and Metrology for Large Optics*, *Proc. SPIE* **966**, 74-81 (Aug. 1988).
5. L. N. Allen and R. E. Keim, "An ion figuring system for large optic fabrication," *Proc. SPIE* **1168**, 33-50 (Aug. 1989).
6. T. J. Wilson, "New technologies fabricate large aspheres," *Laser Foc. World* **26**(9), 111-123 (1990).
7. L. N. Allen, R. E. Keim, T. S. Lewis, and J. Ullom, "Surface error correction of a Keck 10 m telescope primary mirror segment by ion figuring," *Proc. SPIE* **1531**, 195-204 (July 1991).
8. L. N. Allen, J. J. Hannon, and R. W. Wambach, "Final surface error correction of an off-axis aspheric petal by ion figuring," *Proc. SPIE* **1543**, 190-200 (July 1991).
9. S. R. Wilson and J. R. McNeil, "An update on progress in ion beam figuring," in *Proc. Optical Society of America Wkshp. on Optical Fabrication and Testing* (Oct. 1992).
10. C. M. Egert, "Roughness evolution of optical materials induced by ion beam milling," *Proc. SPIE* **1752** (1992).
11. J. Yoshioka, K. Koizumi, M. Shimizu, H. Yoshikawa, M. Miyashita, and A. Kanai, "Ultraprecision grinding technology for brittle materials: application to surface and centerless grinding processes," in *Proc. Milton C. Shaw Grinding Symp. ASME* **16**, 209-227 (1985).
12. T. G. Bifano, T. A. Dow, and R. O. Scattergood, "Ductile regime grinding: a technology for machining brittle materials," *J. Eng. Ind.* **113**, 184-189 (1991).
13. T. G. Bifano and S. C. Fawcett, "Specific grinding energy as an in process control variable for ductile regime grinding," *Precision Eng.* **13**(4), 256-262 (1991).
14. T. G. Bifano, W. K. Kahl, and Y. Yi, "Fixed-abrasive grinding CVD silicon carbide mirrors," *Precision Eng.* **16** (Jan. 1994).
15. S. C. Fawcett and R. W. Rood, "Ion figuring system for segmented, adaptive optics," in *Proc. American Society for Precision Engineering Ann. Mtg. Conf.*, pp. 244-247 (Oct. 1992).
16. H. R. Kaufman, P. D. Reader, and G. C. Isaacson, "Ion sources for ion machining applications," *AIAA J.* **15**(6), 843-847 (1977).
17. N. J. Brown, "Some speculations on the mechanics of abrasive grinding and polishing," in *4th Int. Precision Engineering Semin.*, Cranfield, UK (1987) (also in UCRL Document—96159).



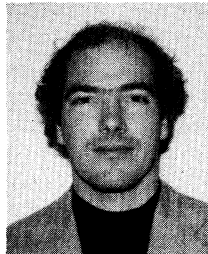
**Steven C. Fawcett** received his PhD in mechanical engineering from North Carolina University in 1991. His primary research was in precision fabrication of optical materials. He has extensive experience in ion fabrication techniques, single-point diamond turning, optical metrology, ductile regime grinding, and sensor and actuator development. Dr. Fawcett spent the last year developing adaptive optical components and optical manufacturing

techniques to support the SELENE laser power beaming program. His current research is centered on producing a replicated mirror prototype for the Advanced X-ray Astronomical Facility S mission. Other projects include funded research into adaptive optical systems and ion figuring techniques for optical components. At his previous position at the Precision Engineering Center at North Carolina State University, Dr. Fawcett was involved with numerous investigations in the area of precision manufacturing. Dr. Fawcett's research efforts have produced seven refereed journal publications and 10 conference presentations.



**Thomas W. Drueding** received a BS in aerospace engineering and an MS in electrical engineering, both from Boston University. After achieving his BS, he worked in research involving satellite remote sensing for atmospheric characterization. He returned to Boston University for his MS and contributed to a major project in image processing, specifically medical imaging. He performed extensive work in mathematical deconvolution techniques. Mr.

Drueding is currently working on his PhD in mechanical engineering under the National Aeronautics and Space Administration Graduate Student Research Program. His research is in the area of ion-beam machining of optical components.



**Thomas G. Bifano** received his undergraduate and MS degrees in mechanical engineering from Duke University. He received a PhD, also in mechanical engineering, from North Carolina State University in 1988. After joining the Boston University Department of Aerospace and Mechanical Engineering in 1988 as an assistant professor, Dr. Bifano established a research program in ultraprecision machining of ceramics and glasses. With the

support from the National Science Foundation, Oak Ridge National Laboratory, and various industry sponsors, he has continued to build on this program in the past 5 years, exploring chemomechanical effects in micromachining, molecular dynamic models of nanoindentation, grinding of ultrathin quartz wafers, machining of ceramic mirrors, ion-beam fabrication, and ductile regime grinding.